Variability of Wind Sea and Swell Waves in the North Atlantic Based on ERA-40 Re-analysis

Alvaro Semedo[1,2]

Kay Sušelj[3]

Anna Rutgersson[1]

[1] Department of Earth Sciences – Meteorology
Uppsala University
Uppsala – Sweden
E-mail: alvaro.semedo@met.uu.se

[2] Risø - DTU National Laboratory for Sustainable Energy
Technical University of Denmark
Roskilde - Denmark

[3] ForWind, Center for Wind Energy Research
Carl von Ossietzky University
Oldenburg - Germany

Abstract

This study presents a qualitative assessment of the wave field in the North Atlantic (NA) basin, based on the ERA-40 wave re-analysis from the European Centre for Medium-Range Weather Forecasts (ECMWF). The wind sea and swell significant wave heights and mean wave lengths, seasonal and geographic distributions, are studied. The geographic distribution and dominance of wind sea and swell waves over the basin, in the winter and in the summer, are also studied. It is shown that the wave field in the NA basin is mostly swell dominated, especially in the summer. The seasonality of the NA wave field is compared with the North Pacific. The qualitative characteristics of the wave fields in both basins is shown to be different. The centers of action of the wind sea and swell significant wave heights are identified using empirical orthogonal function (EOF) analysis.

Keywords: Wave climate, significant wave height, wind sea, swell, North Atlantic.

Nomenclature

H_s = significant wave height

H_s^w = significant wave height of wind sea

H_s^s = significant wave height of swell

T_m = Mean wave period

T_m^w = Mean wave period of wind sea

T_m^s = Mean wave period of swell

L_m = Mean wave length

L_m^w = Mean wave length of wind sea

L_m^s = Mean wave length of swell

θ_m = mean wave direction

θ_m^w = mean wave direction of wind waves

θ_m^s = mean wave direction of swell

C_p = peak phase speed

T_p = peak period

f = frequency

θ = wave direction

m_0 = *zeroth* moment

$\hat{c}$ = wave phase speed

U_{10} = wind speed at 10 meters

φ = wind direction

u_* = friction velocity

1 INTRODUCTION

Ocean surface waves are one of the most obvious and fundamental phenomena present at the air-sea interface. In terms of energy the ocean wave spectrum is dominated by surface gravity waves [1], accounting for more than half of the energy carried by all waves in the ocean surface, and surpassing the contribution of tides, tsunamis, coastal surges, etc. [2].

There are two types of waves in the ocean surface. During the generation and growing processes, they are designated as wind sea. As waves propagate away from their generation area, or when their phase speed is higher than the wind speed, they are called swell. Swell waves are known to travel long distances across the globe, or even across ocean basins [3], with very little attenuation [4-6]. Wind sea waves are generated locally, and receive momentum from the wind in their growing process, therefore they are strongly coupled to the local wind field. On the other hand swell waves are generated remotely and no longer receive momentum from the local wind in order to grow, and are not directly coupled to the local wind field. For this reason waves do not necessarily reflect the local wind field characteristics. Since swell propagates from one place to the other, the local wave field is affected by both local and remote wind forcing. In the open ocean the wave field at a given time and place is, therefore, the result of contributions from waves with different frequencies and directions, reflecting different origins. Higher frequency waves (wind sea) are generated locally, and lower frequency waves (swell) are generated remotely. As a rule of thumb, the longer the frequency, the further swells were generated [2].

The motivations and concerns behind previous studies of wind sea and swell waves have been different. The generation and growth of waves has been the main focus of the wave modeling community, in view of the development of wave models, mainly for forecasting purposes. Since swell waves carry most of the wave energy in the ocean surface, so far the main concern has been its impact on offshore and coastal infra-structures. Recently there has been a renewed interest in the study of swell, ranging from swell propagation and attenuation [7], to the swell impact in the marine atmospheric boundary layer [8-10].

Having in mind the different natures and impacts of wind sea and swell waves, [11] and [12] complemented existing wave climatologies (e.g. [13] and [14]), by separating the global wave climate in the two wave regimes. The study from [11] used a 10 years long data set, obtained from a combination of remote sensing and model hindcast data, and [12] used a 40 years long time series of wave observations from voluntary observing ships (VOS). These studies, although complementary, used different wind sea-swell classification schemes. The methods used for the retrieval of the most common wave parameter, the significant wave height H_S were also different and based on empirical assumptions. Additionally, one of the most important questions concerning the reliability of the VOS wave data is, in fact, the uncertainty of the separation between wind sea and swell, which is dependent on the human observer subjective judgment and experience – the *sailor's eye*. In the open ocean H_S varies gradually over the sea surface and throughout the seasons. The main question is how the variations of H_S^w and H_S^s are related to the variations of H_S. The best way to describe the variability of H_S^w and H_S^s is through wave spectra, which are only available globally, and with a long enough time series, from wave model results, like the European Centre for Medium-Range Weather Forecasts (ECMWF) ERA-40 wave re-analysis [15] . In this study we present a qualitative study of the wave field in the north North Atlantic (NA) basin. The winter and summer climates of H_S^w and H_S^s, and θ_m^w and θ_m^s are studied, based on ERA-40. Taking advantage of the flexibility of the ERA-40 data set, the contribution of the two wave regimes to the seasonal and spatial distributions of H_S is presented. The spatial and seasonal patterns of wind sea and swell predominance are also studied.

Empirical orthogonal function (EOFs) analysis is used to obtain the main variability modes of the H_S^w and H_S^s in the NA, in the winter and in the summer.

The remainder of this paper is organized as follows. Section 2 details the data and methods of analysis. Section 3 presents the wind sea and swell significant wave height winter and summer climates and correspondent variability. The paper is closed with some brief concluding remarks in section 4.

2 DATA AND METHODS OF ANALYSIS

2.1 ERA-40

Although rather close to reality, the analysis produced in operational forecast centers suffers from inhomogeneities. Weather (and wave) forecast models and the analysis procedures are continually improved. Therefore the variability in the analyses archived data is dominated by model and data assimilation changes, rather than by natural variability, making them unsuitable for climate or variability studies. The aim of the re-analysis is to overcome the inhomogeneity problems related to model changes. The best available model and data assimilation scheme, that do not change in time, are used to repeat the analysis procedure for the past, using all the available observations. A re-analysis yields, therefore, a complete global gridded data set, that is as temporally homogeneous as possible. Unfortunately, inhomogeneities due to uneven data coverage and changes in observation systems still remain [16].

The ERA-40 data set is a re-analysis of meteorological observations from September 1957 to August 2002 (45 years), produced by the ECMWF. The data set consist of 6-hourly fields (at synoptic times) with a 1.5ºx1.5º grid resolution, covering the whole globe. Besides global atmospheric variables, it also includes wave parameters. The re-analysis was produced using the ECMWF Integrated Forecasting System (IFS) – a two-way coupled atmosphere-wave model system. The ERA-40 is the first global re-analysis produced using a wave model coupled to a general circulation model. The wave model used in the coupled system is the state-of-the-art third generation WAM model, developed by the Wave Modeling group [17]. Details about the WAM model at ECMWF (the EC-WAM) can be found in [18] and [19]. Additional details about the ERA-40 wave reanalysis are given by [14].

2.2 Wave parameters

The WAM model output is the two-dimensional wave energy spectrum $F(f,\theta)$, obtained at each grid point by integrating the so called wave energy balance equation [20]. In its continuous form, $F(f,\theta)$ describes how the mean sea-surface elevation variance, due to the presence of waves, is distributed as a function of f and θ. From these spectra several derived integrated wave parameters can be obtained. Besides these parameters U_{10} and φ are also used in this study. The mean variance of the sea-surface elevation (the *zeroth* moment) is statistically related to H_s, and is defined as $H_s = 4\sqrt{m_0}$, where $m_0 = \iint f^0 F(f,\theta)dfd\theta$. The T_m used in the present study is the mean wave period from the first moment, based on the first order momentum of the sea surface elevation ($m_1 = \iint f^1 F(f,\theta)dfd\theta$) and is defined as $T_m = m_1 / m_0$. The mean wave lengths are computed from T_m, where, from linear theory, $L_m = 1.56T_m^2$. By weighting $F(f,\theta)$, θ_m is defined in the WAM model as $\theta_m = a\tan(SF/CF)$, where the weights are defined as $SF = \iint sin(\theta)F(f,\theta)dfd\theta$ an $CF = \iint cos(\theta)F(f,\theta)dfd\theta$. The significant wave heights, mean periods, and mean wave directions of the wind sea and swell waves are computed by separating the one-dimensional (1D) spectrum into wind sea and swell components. The separation frequency is defined as the frequency corresponding to the wave phase speed $\hat{c}$ where $1.2 \times 28 \times (u_* / \hat{c}) cos(\theta - \varphi) = 1$. The wind sea and the swell integrated parameters (in the present case m_0 and m_1) are computed by integrating over the respective 1D spectral parts. The peak wave phase speed, as derived from linear theory, is $c_p = gT_p / 2\pi$.

2.3 Methods of analysis

The gridded wave (H_s, H_s^w, H_s^s, T_m, T_m^w, T_m^s, θ_m, θ_m^w, θ_m^s, and T_p) and atmospheric parameters (U_{10}, φ) are processed to yield mean seasonal values, for winter and summer. Winter and summer are considered here as December, January and February (DJF), and June, July, and August (JJA), respectively.

The zonal averaging of H_s, H_s^w, and H_s^s is done from the equator to 70°N. The Black sea, the Mediterranean Sea, and the Baltic Sea, are not taken into account in this averaging to avoid possible biases due to their particular wave regimes. The North Sea and the gulf of Mexico are nevertheless included, since they have a more open communication with the open ocean wave field. The wave age criterion C_p / U_{10} is used to assess the wind sea (or swell) dominance in the wave field. According to this criterion the wave field is considered wind sea dominated if $C_p / U_{10} < 1.2$ and swell dominated if $C_p / U_{10} > 1.2$ [21] and [22]. The wave age $C_p / U_{10} = 1.2$ separation criterion roughly coincides with the friction velocity dependent criterion $C_p / u_* \simeq 33$.6, used by the WAM model. We chose not to include the weighting $1/cos(\theta_m - \varphi)$ as in the WAM model, since in certain areas, when the angle $\theta_m - \varphi$ is high (close to 90°), this weighting factor produces unrealistically high wave age values. Since taking the time average of C_p / U_{10} geographic distribution will smooth the peaks, and since the goal here is to distinguishing which areas of the NA are dominated either by lower or high values of C_p / U_{10}, a probabilistic (frequency of occurrence) approach is used. The probability of a wind sea dominated wave field is defined as $P(C_p / U_{10} < 1.2)$, and the inverse, i.e., the probability of a swell dominated wave field, is defined as $P(C_p / U_{10} < 1.2)$.The probabilities are computed for each grid point and for each 6-hours set.

3 WIND SEA AND SWELL IN THE NORTH ATLANTIC

The combination of storm frequency, duration, and intensity, and the geographic characteristics of the ocean basins, determine the properties of its wave field and seasonal variation. The relatively narrow geometry of the Atlantic Ocean restricts the propagation of Southern Ocean swell into the Northern Hemisphere. Therefore waves in the NA are highly seasonal, and peak in the winter. The primary wave generation area in the NA is along the prevailing extratropical storms track [3], from the East coast of North America towards the Norwegian Sea. This can be seen in figure 1, along the highest values of U_{10}. In this figure the winter and summer yearly averaged U_{10} spatial distribution over the NA is shown. The maximum mean winter value is 12 m/s, and occurs South of Greenland, at ~48°N. The maximum mean summer value is substantially lower (~8.25 m/s), and is located South-South-West of Iceland at ~55°N. In the horse latitudes, north of the

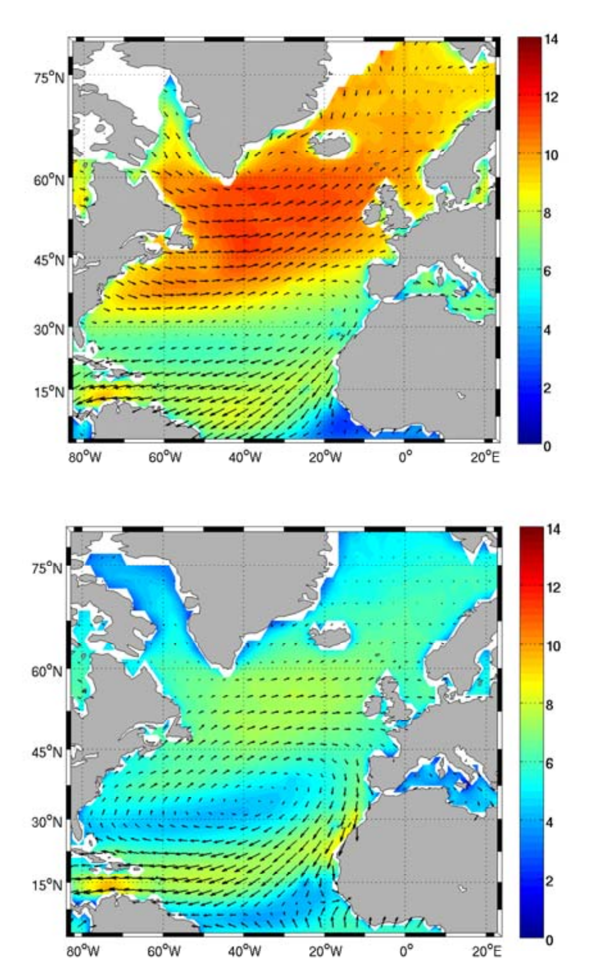

Figure 1: Winter (top) and Summer (bottom) mean U_{10} in ms^{-1} and φ (arrows) in the NA.

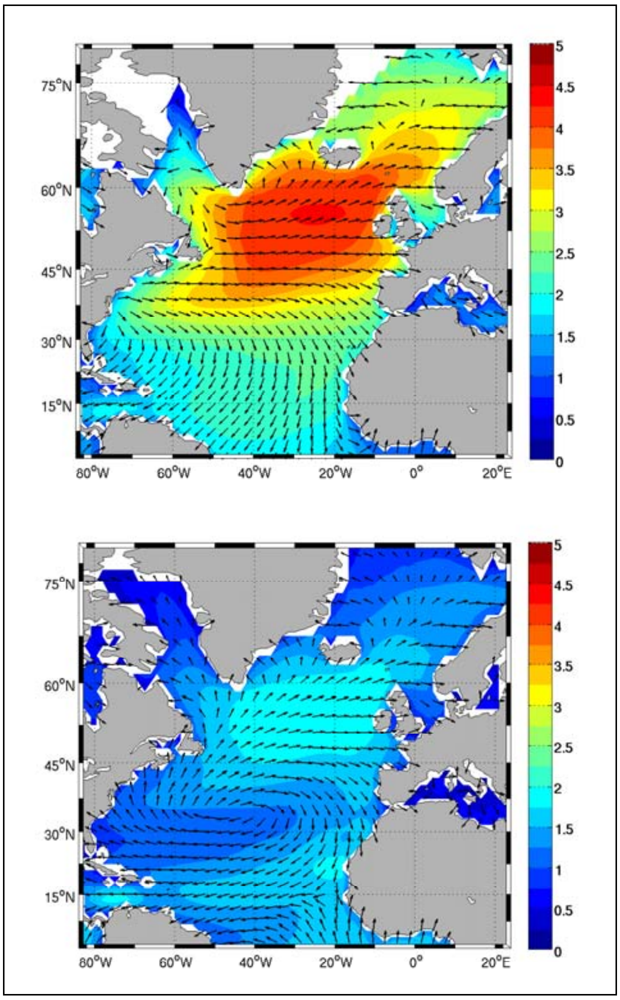

Figure 2: Winter (top) and summer (bottom) mean H_s in m and θ_m (arrows) in the NA.

trade winds (henceforth designated just as trades), U_{10} values are lower, particularly in the summer. In this season the lowest values of U_{10} are in the horse latitudes area and close to the equator. Across the trades the wind speed is consistently in excess of 7 m/s during both seasons.

The spatial yearly averaged distributions of H_s in the winter and in the summer are shown in figure 2. The distribution of the winter and summer H_s follows, to a certain degree, the patterns of U_{10} shown in figure 1. Nevertheless the H_s maximum mean winter value (4.25 m) occurs East on the U_{10} maximum, South of Iceland at ~55°N. This situation occurs most likely because swell generated in the windiest spot propagated towards Iceland. The sum of this swell and locally generated wind sea waves gave rise to the H_s winter maximum. The maximum mean summer value of H_s (less than 2 m) is distributed over a large area between Ireland, Iceland and Greenland. The difference between the mean summer and winter maxima (more than 2 m) reflects the high seasonality of the significant wave height over the NA basin.

It is of no surprise that yearly averaged spatial distributions of H_s^w and θ_m^w, both in winter and summer, are highly coincident with U_{10} and φ for the same periods, as can be seen in figure 3. The reader is advise that the colorbar scale in figure 3 is different than the one in figure 2. The maximum mean winter value of H_s^w (in excess of 2.25 m) is distributed along a large patch, in the centre of the extratropical NA. This area is located from ~45°N to South Greenland and Iceland, and to the West coasts of Ireland and Scotland.This patch is coincident with the mean winter maxima areas of U_{10}, and with the predominant extratropical storm track in the NA, where waves are predominantly generated. Close to the West coasts of Ireland and Scotland the values of H_s^w are still relatively high, which is related to the high values of U_{10} in that area during the winter. In the South-West Europe, off the Iberian Peninsula coast, the values of H_s^w are lower. As we move South, the values of H_s^w gradually decay, following the U_{10} pattern. The low values of U_{10} across the horse latitudes are related to the also low values of H_s^w, in both seasons. Coinciding with the trades, in the tropical NA, there is a well defined patch of 0.75 m high H_s^w, also in both seasons. In the summer, when the extratropical NA is predominantly under the influence of the Azores high, the wind speed drops considerably, compared with the winter season. The values of H_s^w also decrease in that area. In the winter the area covered by the maximum mean winter values of H_s^s is more widely distributed, in the central NA basin, at ~40°N, and propagating South, parallel to the Iberian Peninsula and the North African West coast. Also parallel to the coast of Africa, but more South, a patch of 1.75 m H_s^s can be seen. These swells were originated in the extratropical South Atlantic (SA), and propagated North.

At this stage the question that arises is how predominant is one wave regime over the other, i.e., which wave regime, wind sea or swell, dominates over

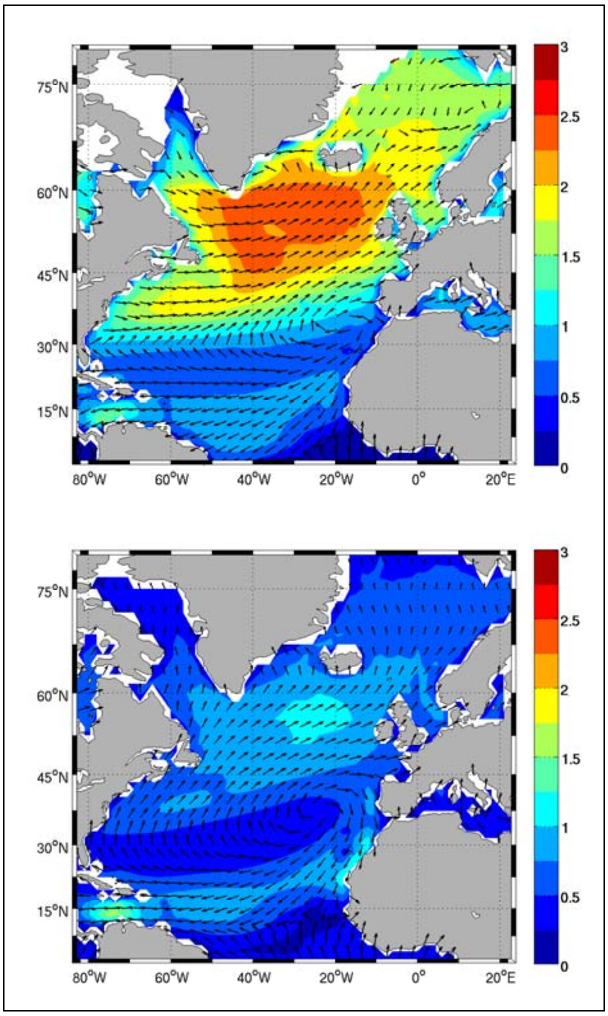

Figure 3: Winter (top) and summer (bottom) mean H_s^w in *m* and θ_m^w (arrows) in the NA.

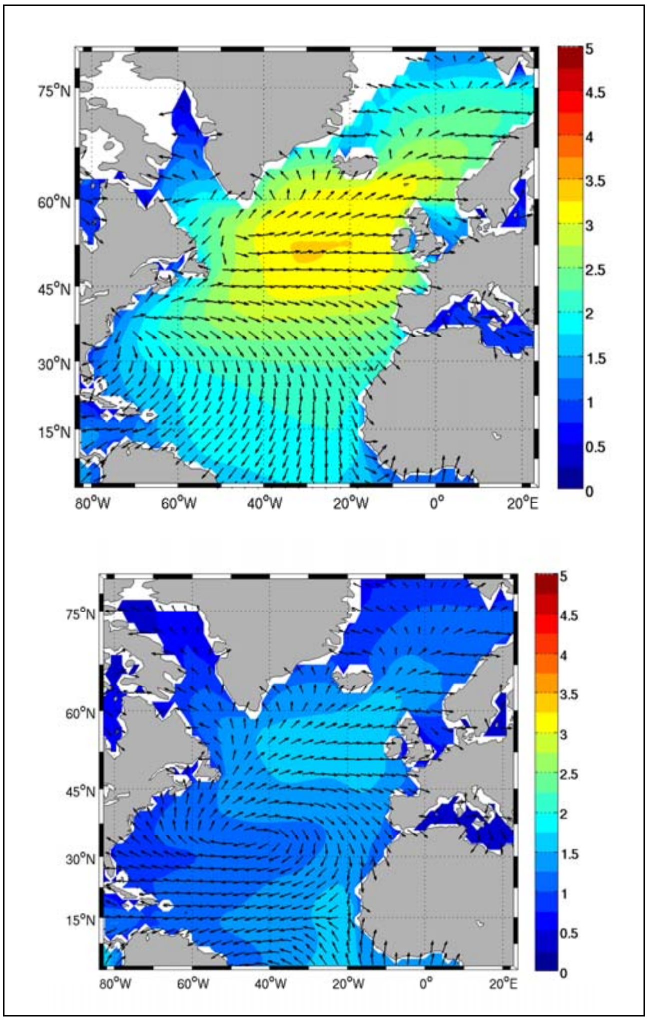

Figure 4: Winter (top) and summer (bottom) mean H_s^s in *m* and θ_m^s (arrows) in the NA.

compared to H_s^w. As can be seen in figure 4, from 35°N up to Greenland and Iceland , the values of H_s^s fall within the 2.5-3.5 m range. The West coasts of Europe, from the Iberian Peninsula to Norway, have higher values of H_s^s compared to the East coast of North America. This is related to the predominant propagating direction of swell towards the East, away from the storm track wave generation area. As with H_s^w, in the summer the spatial distribution of H_s^s is also more uniform than in the winter. The areas of maximum mean summer values of H_s^s are still quite sprawled, with a branch of 1.25 m high swell evolving the other and how this dominance is distributed. As can be seen in figures 5 and 6 the NA basin is mostly swell dominated. The reader is advised that the colorbar scale in different in these two figures. The degree of this dominance is, nevertheless, seasonal, and has also a clearly defined spatial variance. In the winter, over the predominant extratropical storm track, the wind sea dominance is higher than in the summer. In the coastal areas of East North America, and in the fringes of the ocean ice areas off East and West coasts of Greenland, this dominance is close to 50%, reflecting the high wind speed in those areas. In the Southern part of the basin, even across the trade wind area, the wind sea dominance is very low, tending to almost zero towards the equator, and reflecting the light winds regime there.

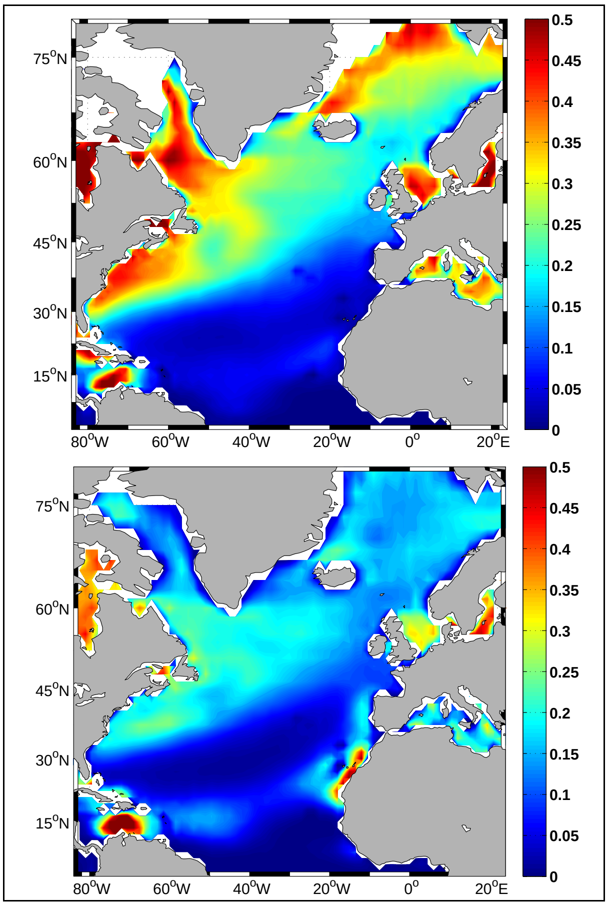

Figure 5: Winter (top) and summer (bottom) probability of having a wind sea dominated wave field.

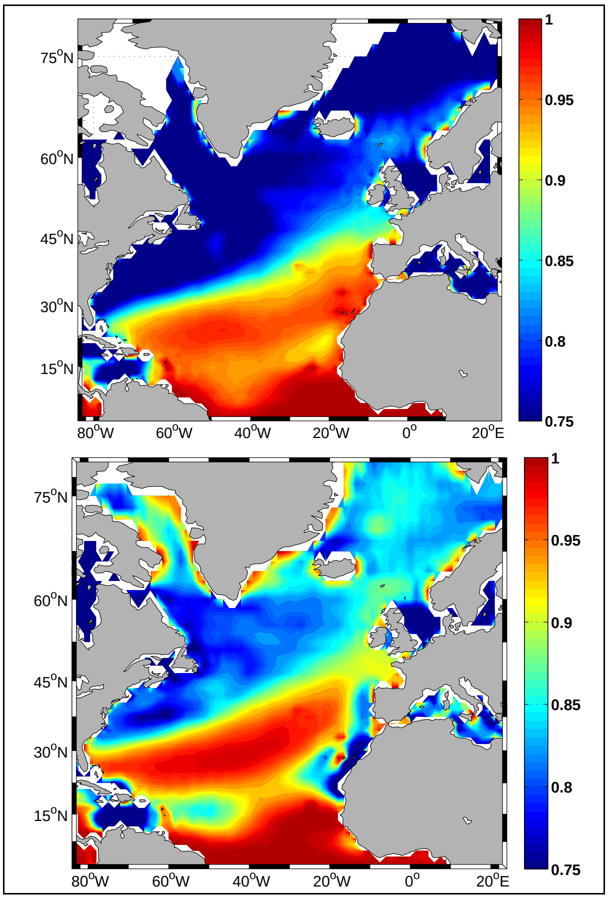

Figure 6: Winter (top) and summer (bottom) probability of having a swell dominated wave field.

In the Summer the probability of having a wind sea dominated wave field is lower over the storm track area. No significant changes occur in the Southern part of the basin. Even in the winter, the probability of swell dominance is almost always higher than 70% over the all basin, as can be seen in figure 6. It is lower along the extratropical storm track, but still higher than the probability of wind sea dominance for the same period. The probability of swell dominance increases to values higher than 90% South of this area. In the summer the swell dominance increases to even higher values, since U_{10} decreases almost over the all basin. Also in the summer, off the coast of the Iberian Peninsula and the West coast of Morocco, the swell dominance is not as high as in other areas. This is due to the mesoscale coastal wind features mentioned before. The tropical storm activity off the Gulf of Mexico also produces a less dominated swell wave field there. There is a sharp transition, producing almost a *sea saw* feature in the NA, between the probability of swell dominance over the extratropical storm track and the Southern part of the basin.

The yearly averaged spatial distributions of the winter and summer L_m^w and L_m^s are shown in figures 7 and 8. The reader is advise that the colorbar scale in figure 3 is different than the one in figure 2. This parameter is of great important, for wave energy purposes, since some wave energy power devices are tuned to be in resonance with the waves length. Therefore the climatological knowledge of L_m^w and L_m^s is crucial, since swell waves carry most of the energy in the wave spectra, as seen from the differences between H_s^w and H_s^s. The longest winter wind sea waves (in excess of 50 m) are located along the wave generation area, coinciding with the NA extratropical storm track. This area extends from the west coast of the North America continent, all the way to the Norwegian sea. Although weaker in the winter, in the trade winds latitudes L_m^w has a regional maxima there (~30 m). In the summer, the NA wind sea mean wave length exhibits a quasi-symmetric tripole, with longer wind sea waves in the extratropical and subtropical areas. Following the eastward wave propagation tracks, the longest winter swells cover a wider area than the wind sea. The longer swells are located west of Ireland (~170 m). The patch of longer swells (in excess of 150 m) covers almost the all multitudinal NA, extending from North Africa to the North Sea. In the Summer, the pattern of L_m^s is more complex reflecting the combination of NA and SA swells, generated in the southern extratropical latitudes, as can be seen by θ_m^s. These long swell waves are located in the Easter part of the NA basin, along the tropical west coast of Africa and the west coast of Europe.

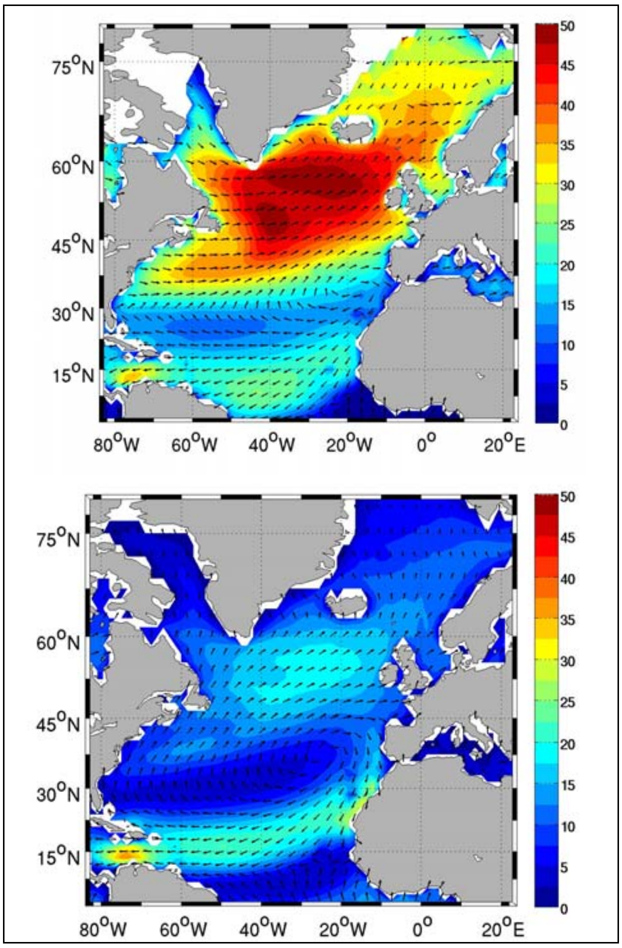

Figure 7: Winter (top) and summer (bottom) mean L_m^w in m and θ_m^w (arrows) in the NA.

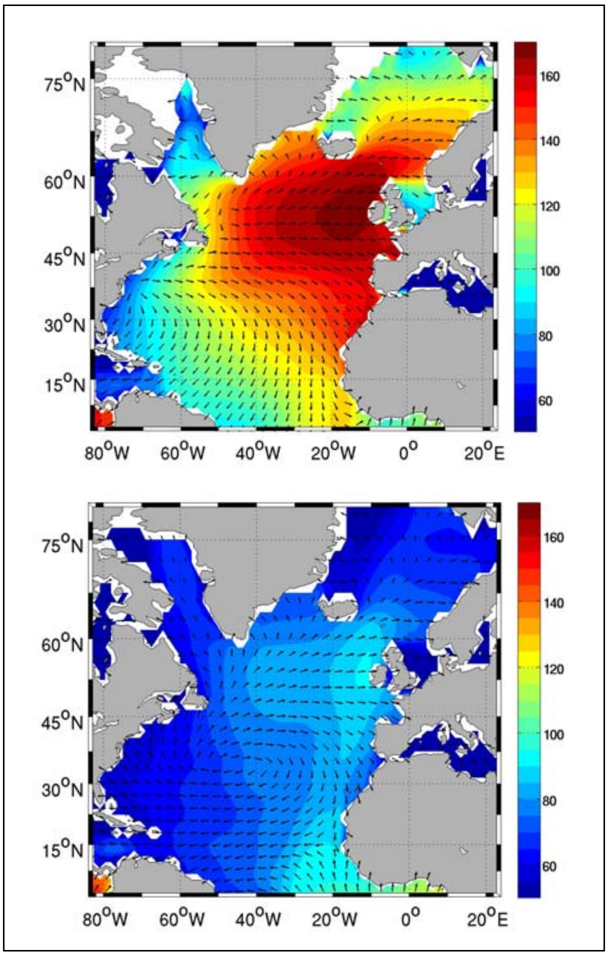

Figure 8: Winter (top) and summer (bottom) mean L_m^s in m and θ_m^s (arrows) in the NA.

As mentioned in the earlier in this section, and shown in figures 1-6, H_s, H_s^w and H_s^s in the NA have a very high seasonality. This seasonality has also a strong North-South geographic signal. In figure 9 a North-South cross section of H_s, H_s^w and H_s^s is shown. These meridional profiles (henceforth designated just as *profiles*) are the result of a zonal averaging of the H_s, H_s^w and H_s^s H_s^s fields in the winter and summer. A similar averaging was done for the North Pacific (NP). The NP profiles are shown in the same figure for comparison purposes with the NA profiles. As expected, the seasonality of the wave field characteristics in the NA is also reflected in the significant wave heights profiles. The H_s is higher in the winter than in the summer over the all NA. It peaks in the winter, along the extratropical latitudes (~52°N), reflecting the high wind speed regime across the storm track, which occurs around that latitude. In the summer the situation is rather different. As a consequence of a weaker extratropical storm activity in the NA H_s is almost even from North to South, with small peaks in the extratropical and trades latitudes. When looking at the H_s^w and H_s^s profiles, their seasonal and North-South variability has particular characteristics that allow a more qualitative view of the wave field over the NA. In the winter the values of H_s^w and H_s^s have peaks around the same latitude for the same reasons as

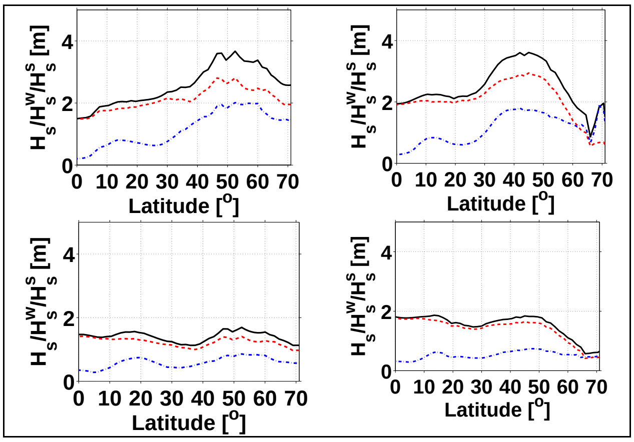

Figure 9: H_s (black), H_s^w (blue) and H_s^s (red) meridional variation. North Atlantic (right plots, top winter, and bottom summer) and North Pacific (left plots, top winter, and bottom summer).

H_s. Around ~30°N (the horse latitudes, roughly north of the trades) where the U_{10} is weak almost all year round, H_s^w has rather low values. Therefore H_s^s is the main contributor for the H_s field there. As we move South towards the equator, the H_s^w profile shows a slight increase, coinciding with the trade winds area. This increase is not present in the winter H_s^s profile, which decreases almost consistently from the extratropical latitudes to the equator. South of the trades, H_s^w decreases, with a minimum value at the equator, where the relative weight of H_s^s in the overall H_s is highest. In the summer, in spite of the relative meridional constancy of H_s, the behavior of the H_s^w and H_s^s show interesting features. The wind sea and swell also peak in the extratropical latitudes, following the (small) H_s increase there. At the trades latitude H_s^w increases, and then decreases as we move South. The minimum value of H_s^w can be seen around 5°N, and South of this latitude H_s^w increases slightly. This minimum roughly coincides with the JJA intertropical convergence zone (ITCZ). In the summer the H_s^s profile also shows a decrease from the extratropical latitudes to the horse latitudes, but now this decrease is less pronounced than in the winter. As in the winter, in the horse latitudes the H_s^s is also dominant. As we move South, the H_s^s values increase, whereas in the winter the profile showed an opposite behavior. This increase in H_s^s is due to the previously mentioned intake of swell that was generated in the Southern extratropical latitudes, and propagated North.

A similar analysis of the NP significant wave heights profiles (also in figure 7) shows the differences between the wave field in that basin, compared to the NA. In the winter the H_s peak value is relatively similar in both basins. The H_s^w profile has a higher peak in the NA extratropical latitudes, reflecting the higher winds there, compared to the NP. But the H_s^s profile in the NA has a lower peak value than in the NP. This slight difference, which allows for H_s to be almost equal in both basins, is the result of the Northbound Southern ocean swell. In DJA (summer in the Southern hemisphere), winds are still rather strong in the Southern extratropical latitudes, and capable of generating waves that propagate as swell towards the the Northern Hemisphere. These swells do not significantly penetrate in the NA basin, but do so in the NP basin, traveling all the way to the NA extratropical latitudes and contributing to the wave climate there. In the summer, as in the winter, in the NP basin is less windy than the NA [14]. Therefore the NP H_s^w profile show that this wave parameter is always lower than in the NA, with lower peaks in both the extratropical and trade winds latitudes. But, due to its geography, the NP is more swell dominated all year round, and therefore the JJA (winter) Southern ocean swell that traveled north allows for higher values in H_s^s at the NP extratropical latitudes and South from there. This fact contributes for a slightly higher peak in the H_s profile in the NP, compared to the NA basin, at the extratropical latitudes, but also in the more South latitudes.

Aiming to explain the different spatial patterns of the wind sea and swell significant wave heights, an EOF analysis is used (see e.g. [23] for details). The principal modes of the H_s^w and H_s^s monthly means, in the

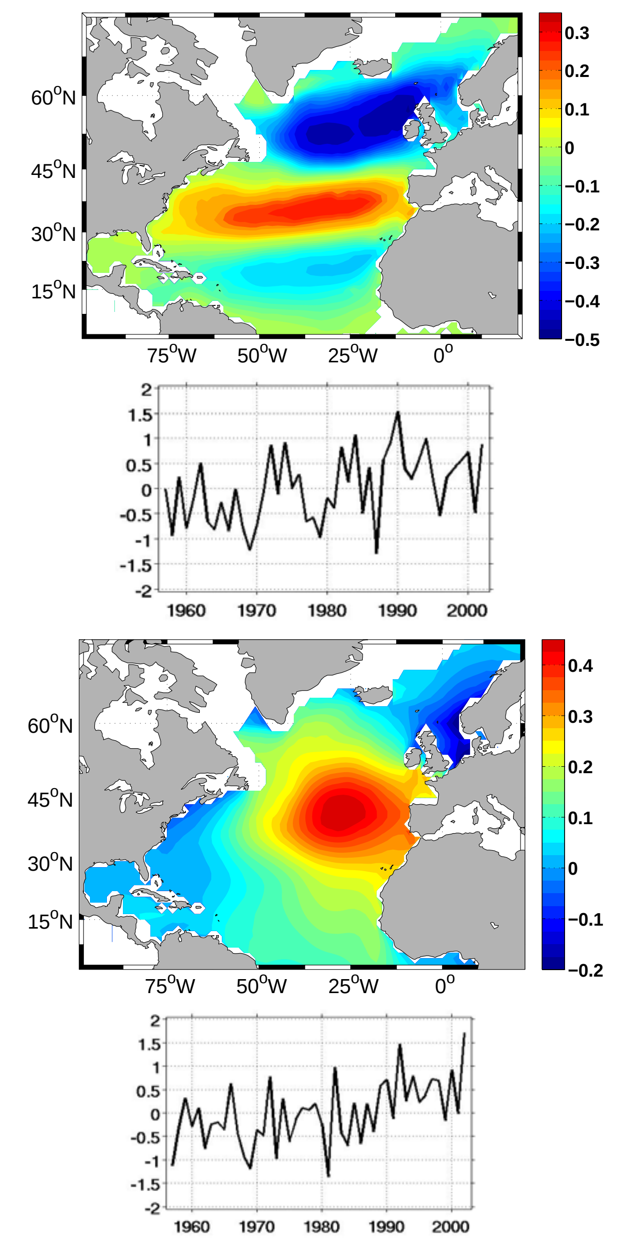

Figure 10: First EOF of winter H_s^W and H_s^S. Spatial distribution and PC1 time series.

winter and in the summer, are investigated. Figures 10 and 11 show the patterns of the first EOFs (EOF1) of H_s^w and H_s^s. To facilitate the inter-season comparison, the EOF1s of H_s^w and H_s^s are organized by seasons in figure 8 (winter) and figure 9 (summer). The reader is advised that the colorbar scale in different in these two figures. The EOF1s of the winter H_s^w and H_s^s (figure 8), explain 20.7% and 60.2% of the spatially averaged variance, respectively. The EOF1 of H_s^w has a very well defined resemblance to the North Atlantic Oscillation (NAO) structure across the central midlatitudinal NA [24], and a statistically significant positive trend in its coefficients time series (PC1). This positive trend can be explained by the persistent positive NAO index trend from the 1960s to the early 1990, indicating an increase in the Westerlies strength, with a direct connection to the wind sea component of the wave field. The maximum of the explained positive variability of H_s^w is located along the predominant extratropical storm track, explaining the predominant wave generation area in the NA. A patch of negative variability is located more South, between 30°-45°N. A slight positive variability is located along the trades, south of the horse latitudes.

The EOF1s of H_s^w and H_s^s in the winter exhibit a noticeable difference. The maxima of the explained variance of swell significant wave height is centered more South, extending all the way to the Iberian Peninsula. This pattern clearly represents swell propagating from the extratropical storm track towards South, and South-South- East. The H_s^s PC1 time series has a positive trend also. This trend is related with the NAO index behavior between 1960 and 1990.

The EOF1s of the summer H_s^w and H_s^s (figure 9), explain 20.8% and 62.5% of the spatially averaged variance, respectively. The maximum of the explained positive variability of the summer H_s^w is located between 30°-40°N, in the center of the basin. A patch of negative variability is located more South, in an area coinciding with the horse latitudes. This negative variability was originated in the west coast of North African and extends West into the center of the NA basins. The highest positive variability is located along the trades, south of the horse latitudes, and North of the equator, where the variability is also close to zero. The summer H_s^w PC1 time series has a slight positive trend until 1976, and a negative trend from then after.

The maximum positive variability pattern of H_s^s, covering an area from 30°N, extending to Greenland and Iceland. It seams like swell waves generated in the center of the basin, along the H_s^w centre of action, have propagated mostly North. The variability South of 30°N is still positive but lower. The summer H_s^w PC1

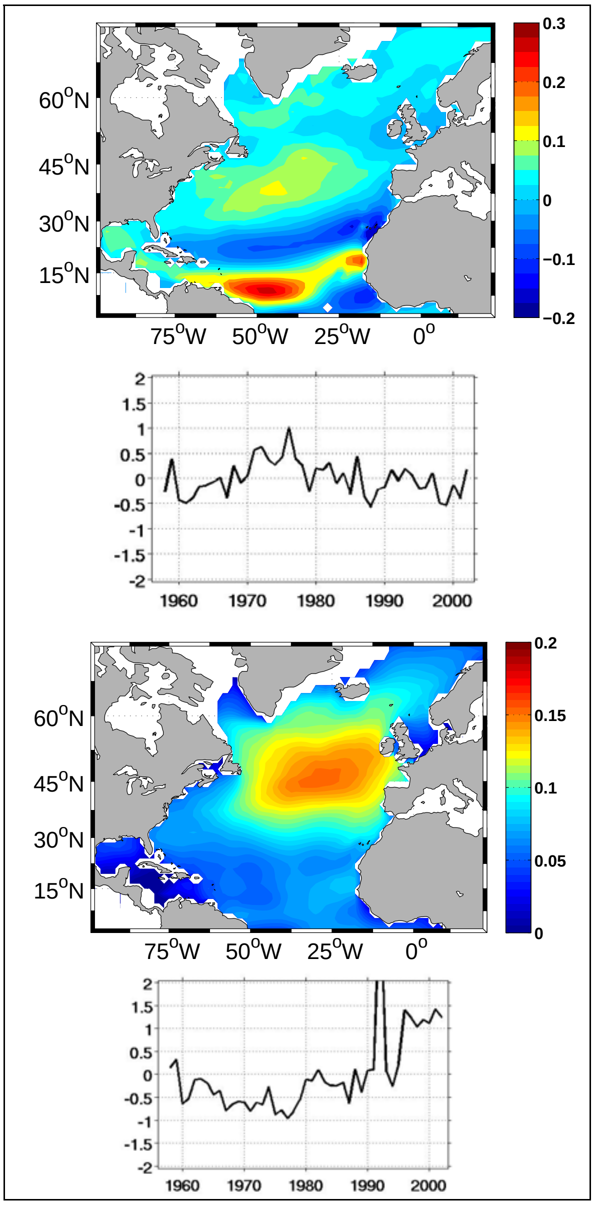

Figure 11: First EOF of summer H_s^w and H_s^s. Spatial distribution and PC1 time series.

time series has a sharp peak in 1992 and 1993. This peak is related to an identified error in the wave height data assimilation in the re-analysis process [14]. The effect of this error on the variability of H_s^s is not investigated in the present study.

4 CONCLUDING REMARKS

A detailed qualitative study of the wave regime in the NA basin, based on the ERA-40 wave re-analysis, was presented. Although several prior studies have characterized the H_s climate in the NA, a more qualitative study of the wave field in that basin, mainly of the wind sea and swell regimes, was missing. The study of the climate and seasonal variability of H_s^w and

H_s^s, and corresponding θ_m^w and θ_m^s, filled this gap. It has been shown how swell dominates the NA basin, even in the winter, when U_{10} peaks and wind waves are more present. The meridional variability of H_s, H_s^w and H_s^s was also studied. The profiles of the significant wave heights showed the high seasonality of the characteristics of the wave regime in the NA.

A rough comparison with the NP H_s, H_s^w and H_s^s climates showed the differences between the wave regimes in both basins, regarding the wind sea and swell regimes. While the H_s climate can be claimed to be relatively similar in the winter and summer, in both basins, their qualitative characteristics are in fact different, due to the differences in the wind speed regime, and to the different geographies of these two basins. The NP is less windy, but it has a considerably stronger Southern Ocean swell intake, compared to the NA. This conclusion is in line with the findings from [3].

The EOF analysis revealed the non surprising conclusion that the wind speed is the dominating source of variability of the wind sea significant wave height. The centers of action of H_s^w and H_s^w are not coincident, showing the main traveling swell path. A more detailed study of the variability of the H_s^w and H_s^s fields, using principal component analysis, in needed, so that the geographic origins of the wind sea and swell across the NA basin can be tracked.

Acknowledgements

Alvaro Semedo and Kay Sušelj were funded by the European Commission through a Marie Curie research fellowship under the ModObs project, contract MRTN-CT-2005-019369. Special thanks are due to Andreas Sterl and Sofia Caires, for valuable suggestions, and to Jean Bidlot, for helping with the access to the ERA-40 data.

References

[1] Munk, W.H., 1951: *Origin and generation of waves*. Proc. First Coastal Engineering Conference, Long Beach, Calif., 1–4.

[2] Kinsman, B. 1965: Wind waves. Prentice-Hall, Englewood Cliffs, NJ, p. 676.

[3] Alves, J.H.G.M, 2006: *Numerical Modeling of Ocean Swell Contributions to the Global Wind-Wave Climate*. Ocean Modelling. Vol. 11 (1-2), 98-122.

[4] Munk, W.H., 1947: *Tracking storms by forerunners of swell*. J. Meterol. 4(2), pp. 45–57.

[5] Munk, W.H., G.R. Miller, F.E. Snodgrass and N.F. Barber, 1963: *Directional recording of swell from distant storms*. Philos. Trans. R. Soc. London, A255, pp. 505–584.

[6] Snodgrass, F.E.,G.W. Groves, K.F. Hasselmann, G.R. Miller, W.H. Munk and W.M. Powers, 1966: *Propagation of swell across the Pacific*. Philos. Trans. R. Soc. London A259, pp. 431–497.

[7] Ardhuin, F. and A. D. Jenkins, 2006: *On the interaction of surface waves and upper ocean turbulence*. J. Phys. Oceanogr., 36, 551–557.

[8] Sullivan, P. P., J. B. Edson, T. Hristov, and J. C. McWilliams, 2008: *Large-eddy Simulations and Observations of Atmospheric Marine Boundary Layers above Nonequilibrium Surface Waves*. J. Atmos. Sci., 65, 1225-1254.

[9] Smedman, A.-S.,, A., U. Högström, E. Sahleé, W. M. Drennan, K. K. Kahma, H. Pettersson, and F. Zhang, 2009: *Observational study of marine atmospheric boundary layer characteristics during swell*. Accepted for publ. in J. Atmos. Sci.

[10] Semedo, A., Sætra, Ø., Rutgersson, A., Kahma, K., Pettersson, H.: *Wave induced wind in the marine boundary layer*. Accepted for publ. in J. Atmos. Sci.

[11] Chen, G., Chapron, B., Ezraty, R., and Vandemark, D., 2002: *A global view of swell and wind sea climate in the ocean by satellite altimeter and scatterometer*. J. Atmos. Oceanic Technol., 19, 1849–1859.

[12] Gulev, S. K., S. K., V. Grigorieva, A. Sterl, and D. Woolf. 2003: *Assessment of the reliability of wave observations from voluntary observing ships: Insights from the validation of a global wind wave climatology based on voluntary observing ship data*. J. Geophys. Res., 108(C7), 3236, doi:10.1029/2002JC001437.

[13] Young I. R., 1999: *Seasonal variability of the global ocean wind and wave climate*. Int. J. Climatol., 19, 931–950.

[14] Sterl, A. and S. Caires, 2005: *Climatology, Variability and Extrema of Ocean Waves - The Web-based KNMI/ERA-40 Wave Atlas*. Int. J. Climatology, 25(7), 963-997, doi:10.1029/joc.1175.

[15] Uppala et al., 2005: *The ERA-40 Re-analysis,* Q.J. Roy. Meteorol. Soc., 131, 2961-3012. 2005

[16] Sterl A., 2004: On the (in-)homogeneity of reanalysis products. *Journal of Climate*, 17: 3866–3873.

[17] WAMDI Group, 1988: *The WAM Model - A Third Generation Ocean Wave Prediction Mode*l. J. Phys. Oceanogr., 18, 1775-1810.

[18] Janssen, P. A. E. M., J. D. Doyle, J. Bidlot, B. Hansen, L. Isaksen, and P. Viterbo, 2002: *Impact and feedback of ocean waves on the atmosphere*. Advances in Fluid Mechanics, W. A. Perrie, Ed., Vol. 1, Kluwer, 155–197.

[19] Janssen, P., 2004: *The Interaction of Ocean Waves and Wind*. Cambridge Univeristy Press.

[20] Komen, G. J., L. Cavaleri, M. Doneland, K. Hasselmann, S. Hasselmann, and P. A. E. M. Janssen, (Eds.) , 1994: *Dynamics and Modelling of Ocean Waves*. Cambridge University Press.

[21] Pierson, W. J., 1964: *The interpretation of wave spectrums in terms of the wind profile instead of the wind measured at a constant height*. J. Geophys. Res. 69, 5191–5203.

[22] Pierson, W. J. and Moskowitz, L. 1964: *A proposed spectral form for fully developed seas based on the similarity theory of S. A. Kitaigorodskii*. J. Geophys. *Res.* 69, 5158–5190.

[23] von Storch, H. and F. W. Zwiers, 1999: Statistical analysis in climatology. Cambridge, Cambridge Univ. Press.

[24] Rogers, J.C., 1984: *The Association between the North Atlantic Oscillation and the Southern Oscillation in the Northern Hemisphere*. Mon. Wea. Rev., 112, 1999-2015.